ELSEVIER

SCIENCE DIRECT®

Physics Letters B 551 (2003) 63–70

PHYSICS LETTERS B

www.elsevier.com/locate/npe

Coulomb breakup of the neutron-rich isotopes ^{15}C and ^{17}C

U. Datta Pramanik [a,b], T. Aumann [a], K. Boretzky [c], B.V. Carlson [d], D. Cortina [e], Th.W. Elze [f], H. Emling [a], H. Geissel [a], A. Grünschloß [f], M. Hellström [a], S. Ilievski [f], J.V. Kratz [c], R. Kulessa [g], Y. Leifels [a], A. Leistenschneider [f], E. Lubkiewicz [g], G. Münzenberg [a], P. Reiter [h], H. Simon [i], K. Sümmerer [a], E. Wajda [g], W. Walus [g]

[a] *Gesellschaft für Schwerionenforschung, D-64291 Darmstadt, Germany*
[b] *Saha Institute of Nuclear Physics, 1/AF Bidhannagar, Kolkata 700064, India*
[c] *Institut für Kernchemie, J. Gutenberg-Universität, D-55099 Mainz, Germany*
[d] *Instituto Tecnologico de Aeronautica, CTA, Sao Jose dos Campos, Brazil*
[e] *Universidad Santiago Compostela, E-15782 Santiago de Compostela, Spain*
[f] *Institut für Kernphysik, J.W. Goethe-Universität, D-60486 Frankfurt, Germany*
[g] *Instytut Fizyki, Uniwersytet Jagelloński, PL-30-059 Kraków, Poland*
[h] *Sektion Physik, Ludwig-Maximilians-Universität, D-85748 Garching, Germany*
[i] *Institut für Kernphysik, Technische Universität, D-64289 Darmstadt, Germany*

Received 4 April 2002; received in revised form 15 July 2002; accepted 31 October 2002

Editor: V. Metag

Abstract

Coulomb breakup of unstable neutron-rich carbon isotopes ^{15,17}C has been studied at energies around $\sim$ 500–600 MeV/nucleon. Non-resonant low-lying dipole strength is observed in these isotopes which can be explained by a direct breakup mechanism. In addition to the decay neutron from excited projectile, γ-rays emitted from excited fragments after Coulomb breakup are measured in coincidence, giving access to quantitative spectroscopic information. The spectroscopic factor deduced for a valence neutron occupying the $s_{1/2}$ level in the ^{15}C ground state is consistent with that obtained earlier from (d, p) transfer reactions. The analysis for Coulomb breakup of ^{17}C shows that most of the cross section yields the ^{16}C core in excited states. The predominant ground-state configuration of ^{17}C is found to be $^{16}\mathrm{C}(2^+) \otimes \nu_{s,d}$.

PACS: 21.10; 23.90.+w; 25.60.-t; 27.20.+n

Keywords: Exotic nuclei; Coulomb breakup

The physics of exotic nuclei has attracted much interest during the past decade [1–3]. In many respects, the properties of nuclei with large neutron excess have turned out to be very different compared to those of stable nuclei. One interesting observation in exotic nuclei is the existence of a strong dipole transition component located just above the neutron separation threshold. Loosely-bound valence nucle-

E-mail address: ushasi@anp.saha.ernet.in (U. Datta Pramanik).

0370-2693/02
PII: S0370-2693(02)03016-2

ons couple strongly to the particle continuum yielding the phenomenon of low-lying multipole strength, not known in stable nuclei. Experimentally, low-lying dipole strength was observed in the halo nuclei ^{6}He [4], ^{11}Li [5–7], ^{11}Be [8], ^{19}C [9], but recently also in the more tightly bound isotopes $^{17-22}$O [10]. To explain the low-lying dipole strength in neutron-rich nuclei, two types of mechanisms have been discussed. One is the excitation of a soft dipole resonance resulting from oscillations of the core against the valence nucleons [11]. The other is the direct breakup mechanism, i.e., a single-particle transition into the continuum, which occurs at large strength due to the spatially extended valence-nucleon wave function [12]. One may observe such excitations by Coulomb breakup induced at near relativistic beam energies. Since a loosely-bound nucleon or a cluster of nucleons has a large probability of being outside the nuclear radius of the more tightly bound core nucleus, large Coulomb dissociation cross sections are expected.

The main purpose of this Letter is to show that the details of the ground-state configuration of loosely-bound nuclei can be derived from excitation of these nuclei into non-resonant continuum states through electromagnetic interaction. There have been many studies of the structure of exotic nuclei using strongly interacting probes (e.g., [13–17]). Studying the structure of loosely-bound nuclei using electromagnetic excitation as a spectroscopic tool has the advantage that this interaction is well understood. Only a limited number of experimental investigations have so far employed Coulomb breakup [8,9]. Here, we present the first study of the single-particle structure of exotic nuclei through Coulomb dissociation by measuring both the decay neutron and γ-rays in coincidence with the projectile. The method is applied to the neutron-rich nuclei ^{15,17}C whose neutron separation energies amount to 1.218 and 0.729 MeV, respectively. The different excited states of the fragments after direct breakup can be identified through their characteristic γ-ray decay. Moreover, the distribution of the Coulomb dissociation cross section $d\sigma/dE^*$ versus excitation energy E^* depends on the quantum numbers of the single-particle orbital occupied by the valence neutron.

The ground state spin of ^{15}C is known to be $I^\pi = 1/2^+$. The spectroscopic factor for the valence neutron in the s orbital is close to one as obtained from ^{14}C$(d, p)^{15}$C reactions. The reported values are 0.99 [18], 0.88 [19], and 1.03 and 0.76 [20], to some extent depending on the choice of the DWBA parameter sets. A narrow momentum distribution (67 ± 3 MeV/c) of the fragment ^{14}C was observed after one-neutron removal [14,17] which is indicative of a spatially extended matter radius. It is interesting to note that the matter radius deduced from interaction cross sections, however, is only marginally larger than that of the core nucleus [21]. On the other hand, the charge-changing cross section for this isotope is larger than that for neighboring carbon isotopes [22]. These somewhat conflicting results encouraged us to investigate the nucleus ^{15}C. The measurement for ^{15}C should also serve to check the new method as presented here, by comparing resulting spectroscopic factors to those from transfer reactions.

The ground state spin of ^{17}C is not fully established experimentally. Since the last valence neutron can occupy the $1s_{1/2}$, $0d_{3/2}$, or $0d_{5/2}$ orbitals, the ground state spin could be either $1/2^+$, $3/2^+$, or $5/2^+$. Shell model calculations predict three close-lying levels with these spins. Warburton and Millener [23] showed that the analysis of the spectra following β-decay of ^{17}C seems to exclude a $5/2^+$ ground state spin. A comparison of the measured β-decay half-life of this isotope [24] with the theoretical prediction for a Gamow–Teller β-decay, however, allows both $3/2^+$ and $5/2^+$ as ground state spin. But the comparison between the experimental one-neutron-removal cross section for ^{17}C and Hartree–Fock calculations including dynamical core polarization favours $5/2^+$ as the ground state spin [25]. It may be interesting to note that though the neutron separation energy is smaller than in the case of ^{15}C, a relatively broad momentum distribution (141 ± 6 MeV/c) of the fragment (^{16}C) was observed after one-neutron removal from ^{17}C [13, 14,17]. The broad momentum distribution could be explained by considering s and d neutrons coupled to the first 2^+ core-excited state of ^{16}C. This was confirmed by measuring the momentum distribution of the core fragment (^{16}C) in coincidence with its γ-decay from the first excited state after one-neutron knockout [26]. There are also several theoretical efforts to study the structure of ^{15,17}C [27–30] which need experimental verification.

In this Letter, experimental results on single-particle properties of ^{15,17}C will be presented. These

are obtained by analyzing electromagnetic excitation cross sections of secondary beams impinging on a high-Z target at energies of ~ 500–600 MeV/nucleon within the direct-breakup model. At such high beam energies, the excitation mechanism favors E1 transitions with only small contributions from E2 transitions.

The radioactive beams were produced by fragmentation of a primary ^{40}Ar beam delivered by the synchrotron SIS at GSI, Darmstadt, impinging on a beryllium target (4.0 g/cm^2). The secondary beams were separated according to their magnetic rigidities using the Fragment Separator FRS [31]. Since no degrader was used, the beam contained various isotopes with similar mass-to-charge ratios ($A/Z = 2.5$–2.75) ranging from beryllium up to fluorine. Among those were ^{15,16,17}C with beam energies of 605, 548 and 496 MeV/nucleon, respectively. The secondary beams were identified uniquely by means of energy-loss and time-of-flight measurements. The trajectories of the particles were measured with position-sensitive silicon diodes placed before and after the secondary target. Behind the target, the fragments were deflected by a large-gap dipole magnet. By using energy-loss and time-of-flight measurements as well as position measurements before and after the dipole magnet, the nuclear charge, velocity, scattering angle, and the mass of each fragment were determined. The positions of the fragments behind the dipole magnet were measured by scintillating fiber detectors [32]. The neutrons emitted from the excited projectiles or excited projectile-like fragments are kinematically focussed into forward direction and were detected with high efficiency in the neutron detector LAND [33]. This detector was placed at zero degree about 11 m downstream from the target and covered a horizontal and vertical angular range of about ± 80 mrad. In order to detect γ-rays, the target was surrounded by the 4π Crystal-Ball spectrometer consisting of 160 NaI detectors.

By measuring the momenta of all decay products of the projectile after inelastic scattering followed by breakup, the excitation energy of the nucleus is determined. The Coulomb dissociation cross section measured with the lead target (1.8 g/cm^2) was obtained after subtracting nuclear contributions determined from the data obtained with a carbon target (0.573 g/cm^2) and applying a proper scaling of the cross sections (for details see [35]). Background contributions from reactions induced by materials of detectors were determined from data taken without any target and were subtracted. The cross section can be experimentally further differentiated by the coincident observation of the characteristic γ-decay transitions of the core fragments. Since the Crystal-Ball spectrometer covers the full solid angle, the γ-ray sum energy can be determined reflecting directly the excitation energy of the excited state. The detection efficiencies of the NaI γ detectors under experimental conditions were estimated by GEANT [34] simulations. Simulated and experimental results from a calibration with a ^{60}Co γ-ray source were found to be in agreement within 4%.

The resulting data are analysed on the basis of the direct-breakup model [9,27] in which the nucleus is considered to consist of a core and a loosely-bound neutron. When a projectile moving with high velocity passes a target of high nuclear charge Z, it may be excited by absorbing virtual photons from the time-dependent Coulomb field. The corresponding differential cross section $d\sigma/dE^*$ for dipole excitations decomposes into an incoherent sum of components $d\sigma(I_c^\pi)/dE^*$ corresponding to different core states with spin and parity, I^π, populated after one-neutron removal. For each core state, the cross section furthermore decomposes into an incoherent sum over contributions from different angular momenta j of the valence neutron in its initial state:

$$\frac{d\sigma(I_c^\pi)}{dE^*} = \left(\frac{16\pi^3}{9\hbar c}\right) N_{\mathrm{E1}}(E^*) \sum_j C^2 S\left(I_c^\pi, nlj\right) \times \sum_m \left|\langle q|(Ze/A) r Y_m^1|\psi_{nlj}(r)\rangle\right|^2. \quad (1)$$

$N_{\mathrm{E1}}(E^*)$ is the number of equivalent dipole photons of the target Coulomb field at an excitation energy E^*, which can be computed in a semi-classical approximation [36,37]. $\psi_{nlj}(\vec{r})$ represents the single-particle wave function of the valence neutron in the projectile ground state and $C^2S(I_c^\pi, nlj)$ its spectroscopic factor with respect to a particular core state (I_c^π). The final-state wave function $\langle q|$ of the valence neutron in the continuum may be approximated by a plane wave. We discuss, however, also the effect of distorted waves. The single-particle wave functions have been derived from a Woods–Saxon potential with a radius parameter $r_0 = 1.25$ fm and diffuseness parameter $a = 0.7$ fm which were used earlier in this mass

region for neutron-rich nuclei [14,16,26]. The depth of the potential is adjusted in order to reproduce the valence-neutron separation energy.

Eq. (1) indicates that the dipole strength distribution is very sensitive to the single-particle wave function which in turn depends on the orbital angular momentum and the binding energy of the valence neutron. Thus, by comparing the experimental Coulomb dissociation cross section with the calculated one, information on the ground state properties such as the orbital angular momentum of the valence nucleon and the corresponding spectroscopic factor may be gained. The core state to which the neutron is coupled can be identified by the characteristic γ-decay of the core after releasing the valence neutron. The Coulomb breakup cross section which leaves the core in its ground state is obtained from the difference between the total cross section and the excited-state(s) contribution(s).

The data analysis for ^{15}C shows that the overwhelming part ($\sim 90\%$) of the breakup cross section leaves the ^{14}C core in its ground state and only a small fraction ($\sim 10\%$) of ^{14}C fragments are found in excited states as could be deduced from the corresponding γ-ray spectra, see Fig. 1. The total Coulomb dissociation cross section for $^{15}\mathrm{C} \rightarrow {}^{14}\mathrm{C} + \text{neutron}$ amounts to 360 ± 10 mb, integrated up to 20 MeV excitation energy. No resonance-like structure is observed. The sum-energy spectrum of the γ-decay from ^{14}C fragments is displayed in the upper part of Fig. 1. It should be noticed that the rise in intensity towards low γ-sum energies is due to atomic processes as we deduce from spectra recorded for projectiles that do not undergo breakup. After subtracting the contributions from excited states, $d\sigma/dE^*$ for electromagnetic excitation of ^{15}C followed by decay into a neutron and a ^{14}C fragment in its ground state is obtained (filled symbols in Fig. 1). The cross section obtained with the carbon target, reflecting essentially nuclear breakup, is shown as well (note that a scaling factor of 2.1 was applied, the ratio of nuclear cross sections for lead and carbon targets [35]) and appears to be very small. The distribution $d\sigma/dE^*$ is shown without acceptance and efficiency corrections for the neutron detector. Instead, the calculated cross sections were convoluted with the detector response obtained from detailed simulations. The experimentally observed shape of the spectrum is in good agreement with the calculated one

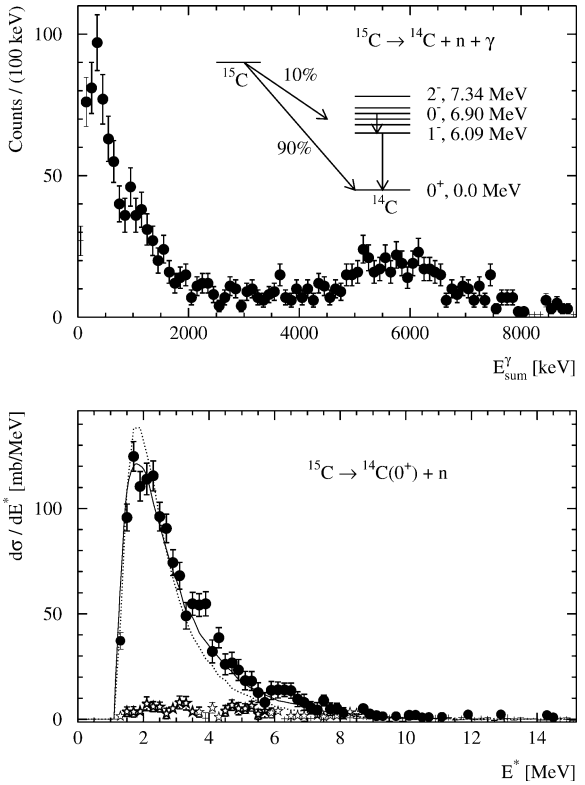

Fig. 1. Top: γ-sum energy spectrum measured in coincidence with ^{14}C fragments after Coulomb breakup of ^{15}C in a lead target. The inset shows a partial scheme of levels in ^{14}C and their population after Coulomb breakup. Bottom: differential Coulomb dissociation cross section with respect to excitation energy (E^*) of ^{15}C breaking up into a neutron and a ^{14}C fragment in its ground state (filled circles). The nuclear contribution (see text) is shown by open symbols. The solid curve displays the result from the direct-breakup model in plane-wave approximation, the dotted curve that from a distorted-wave analysis.

(solid curve in Fig. 1) where an s-wave neutron single-particle wave function coupled to the ^{14}C ground state as initial state and an outgoing plane wave is adopted. From the absolute cross section, a spectroscopic factor 0.73 ± 0.05 is deduced by fitting the calculated differential cross section $d\sigma/dE^*$ to the measured spectrum (see Fig. 1). It is important, however, to notice that this spectroscopic factor would increase to 0.92 ± 0.07, if Woods–Saxon potential parameters of $a = 0.5$ fm and $r_0 = 1.15$ fm were adopted. Such parameters were used in this mass region for stable nuclei and were also adopted by Sauvan et al. [17] for neutron-rich nuclei of similar masses. A distorted-wave approxi-

mation for the neutron in the continuum leads to a spectroscopic factor of 0.97 ± 0.08. For this distorted-wave calculation we used the same Woods–Saxon parameters ($a = 0.7$ fm, $r_0 = 1.25$ fm) for the initial state as were used in the plane-wave approximation above. In the case of the outgoing wave, a real volume and an imaginary surface potential were utilized with geometrical parameters (a and r_0) as most commonly adopted in the literature for neutron–nucleus optical potentials. The real potential depth was taken to be $V = 50.0 - 0.3\,E_n$ (MeV), where E_n is the relative energy between core and the outgoing neutron. The strength of the imaginary surface potential was chosen as $W_s = 7.0 - 0.07\,E_n$ (MeV). The real potential depth is close in magnitude and energy dependence to that of the Wilmore–Hodgson global neutron optical potential [38], which was fitted to low-energy neutron scattering data for heavier nuclei ($E_n < 10$ MeV and $A > 40$) and to that of a more recent fit to neutron scattering data on ^{12}C, ^{14}N, and ^{16}O, by Chadwick and Young [39]. The surface imaginary strength was taken to be intermediate between the more absorptive Wilmore–Hodgson values and the smaller Chadwick–Young values. For all the cases, the strength of the spin-orbit interaction was 7.0 MeV. In Fig. 1, the solid and dotted curves show the calculations within plane and distorted wave approximation, respectively, with adjusted spectroscopic factors. From (d, p) transfer reactions, spectroscopic factors between 0.76 and 1.03 were reported [18–20]. It thus appears that our result obtained from Coulomb breakup is consistent with that from transfer reactions within the systematic uncertainties inherent to both methods. Both results are in good agreement with the shell-model value of 0.98 obtained using the WBP interaction [40]. We notice, however, that the description of our data in distorted-wave approximation is less perfect than that obtained within the plane-wave approximation, see Fig. 1. It appears that more theoretical work is required, which is beyond the scope of this experimental report. In the following analysis we quote spectroscopic factors resulting from both, the plane-wave and distorted-wave approximations.

Aside from the ^{14}C ground state, levels around $E^* \sim 6$ MeV are populated in Coulomb breakup. Due to the intrinsic resolution of the NaI detectors and the Doppler broadening effect, these states cannot be resolved. The spectrum appears somewhat down-shifted in energy due to the detector response. The inset of Fig. 1 shows a partial level scheme of ^{14}C [41]. Among the six excited states in ^{14}C at energies between 6 and 7.35 MeV, in particular the 1^- state at 6.093 MeV and the 2^+ state at 7.01 MeV could in principle be excited by the Coulomb field after the breakup reaction. The cross sections for such excitations, however, are less than 1 mb as estimated from a semiclassical calculation using known reduced matrix elements from the literature [41]. This is negligible compared to the observed cross section of 36 ± 3 mb. Thus, it cannot explain the population of these excited states. The observation of ^{14}C excited states may tentatively be understood as excitation of a more deeply bound neutron of ^{15}C into the continuum. The p-orbital is the least bound level occupied by core neutrons. In ^{14}C, a hole in the $p_{1/2}$ or $p_{3/2}$ orbital may couple with the $s_{1/2}$ valence neutron to $I^\pi = 0^-, 1^-$, and 2^- states. Levels of such structure are found at energies 6.09 MeV (1^-), 6.90 MeV (0^-), and 7.34 MeV (2^-), see inset of Fig. 1. Experimentally, aside from a γ-sum energy peak around 6 MeV, we observe a γ-transition around 1 MeV in the singles γ-spectrum which may be due to the transitions $0^- \to 1^-$ or $2^- \to 1^-$. Furthermore, the Coulomb dissociation cross section taken in coincidence with the γ-sum energy peak around 6 MeV can be well reproduced by the direct-breakup model assuming the excitation of a p neutron. The spectroscopic amplitude for this process, analysed in plane-wave approximation, is in qualitative agreement with that from a shell-model calculation, see Table 1. We note, however, that the distorted-wave approximation delivers a value differing considerably from that of the plane-wave approximation. The difference is conceivable since a dipole excitation of a p neutron yields outgoing s and d waves. The outgoing s-wave penetrates deeper into the nuclear potential and suffers more absorption than p waves or those of higher angular momentum. Again, a final conclusion requires more theoretical work and more systematic experimental data. Nevertheless, it appears that Coulomb breakup, in principle, even allows to probe the structure of more deeply bound nucleons. Our experimental results on ^{15}C are summarized in Table 1.

We now turn to the analysis of ^{17}C. The sum-energy spectrum of the γ decay from ^{16}C fragments after Coulomb breakup of ^{17}C exhibits a strong peak around 1.766 MeV and another peak around 3–4 MeV,

Table 1
Partial Coulomb dissociation cross sections of ^{15,17}C for different core states and valence-neutron orbitals. Cross sections obtained from the direct-breakup model for neutrons occupying s, p, and d orbitals with a spectroscopic factor of one are given for comparison. The cross sections are integrated up to an excitation energy of 20.0 MeV. The corresponding spectroscopic factors from shell-model calculations [26,40] and the ones derived from the experiment are quoted in the last two columns

Isotope	Core state	Neutron orbital	Cross section [mb]		Spectroscopic factor	
	I^π (E; [MeV])		Direct breakup	Experiment	Shell model	Experiment
^{15}C	$0^+(0.0)$	$1s_{1/2}$	437[a]	324 ± 15	0.98	0.73 ± 0.05[b]
			299[c]			0.97 ± 0.08[d]
						0.76–1.03[e]
	$1^-(6.09)$	$0p_{1/2,3/2}$	27[a]	36 ± 3	1.63	1.3 ± 0.1[b]
	$+0^-(6.90)$					
^{17}C	$0^+(0.0)$	$0d_{3/2}$	108[a]	9^{+15}_{-9}	0.03	
	$2^+(1.76)$	$1s_{1/2}$	166[a]	62 ± 7	0.16	0.23 ± 0.08[b]
			90[c]			0.26 ± 0.14[d]
		$0d_{5/2}$	49[a]		1.44	0.6 ± 0.4[b]
			23[c]			1.6 ± 0.6[d]
	~ 3–4			25 ± 7		

[a] Calculation performed in plane-wave approximation.
[b] Spectroscopic factor obtained from this experiment by comparing to calculations in plane-wave approximation.
[c] Calculation performed in distorted-wave approximation.
[d] Spectroscopic factor obtained from this experiment by comparing to calculations in distorted-wave approximation.
[e] Experimental results from (d, p) reactions [18–20].

see Fig. 2(top). In contrast to ^{15}C, Coulomb breakup of ^{17}C yields the ^{16}C core mainly in excited states, i.e., in the $I^\pi = 2^+$ state at an excitation energy of 1.766 MeV with $64 \pm 9\%$ of the cross section and in excited states at energies around 3–4 MeV with $27 \pm 9\%$ of the cross section. Only a small part of the cross section leaves the core in its ground state. In principle, one could argue that the population of the core-excited states could be due to inelastic excitation in a second step after breakup as discussed already for ^{15}C. By inspection of our data from the ^{16}C secondary beam for excitation of such states, it can be shown, however, that this two-step mechanism is negligible. The relative cross sections for the population of different core states are indicated together with a partial level scheme of ^{16}C [42] in the upper part of Fig. 2. The lower part of Fig. 2 shows $d\sigma/dE^*$ for electromagnetic excitation of ^{17}C in coincidence with the 1.766 MeV γ transition (^{16}C$(2^+ \to 0^+)$) after subtracting the contribution of the cascade γ-rays de-exciting the states at 3–4 MeV excitation energy. Similar to ^{15}C, no resonance structure is observed in the Coulomb dissociation spectrum of ^{17}C. The data can be well reproduced by a fit including contributions from wave functions involving $l = 0$ and $l = 2$ neutrons, as shown in Fig. 2 (dashed and solid curves). The spectroscopic factors obtained from the fit to the data using the plane-wave approximation (solid curve in Fig. 2) for neutrons occupying s and d orbitals are 0.23 ± 0.08 and 0.6 ± 0.4, respectively. These values change to 0.26 ± 0.14 and 1.6 ± 0.6, respectively, in the distorted-wave approximation (dashed curve in Fig. 2). Obviously, ^{16}C$(2^+) \otimes \nu_{s,d}$ can be considered as the dominant ground state configuration of ^{17}C and in consequence, a $1/2^+$ ground state spin of ^{17}C can be ruled out. Hence, $3/2^+$ and $5/2^+$ are the possible ground state spins of ^{17}C. Recently, similar results were observed by a completely different method. Maddalena et al. [26] reported that the momentum distribution of ^{16}C fragments in coincidence with the 1.766 MeV γ-ray transition after a knockout reaction agrees well with Glauber model calculations considering s and d valence nucleons with spectroscopic factors from shell-model calculations of 0.16 and 1.44, respectively. The Coulomb dissociation cross section for population of ^{16}C in its ground state is very small ($\sim 9^{+15}_{-9}$ mb). Shell-model calculations [26] quote spectroscopic factors of 0.7

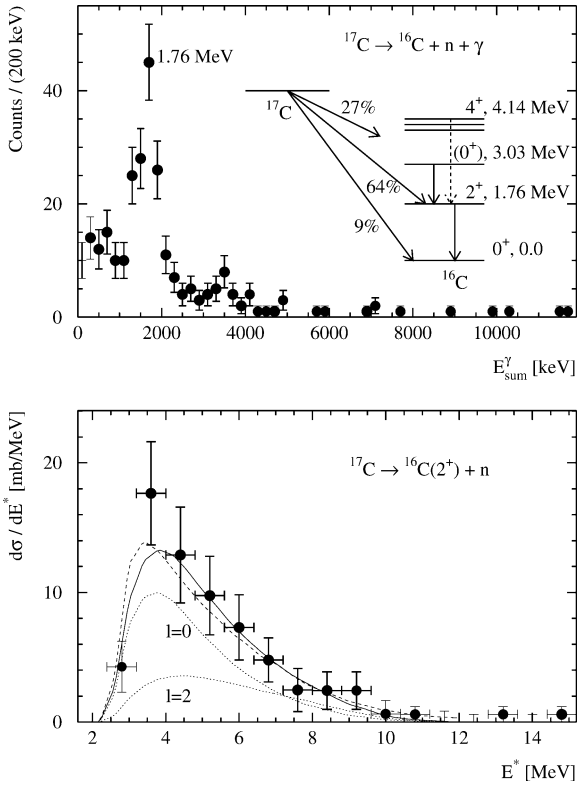

Fig. 2. Top: sum-energy spectrum of γ-decay transitions from ^{16}C after Coulomb breakup of ^{17}C. The inset shows a partial scheme of levels in ^{16}C and their population after Coulomb breakup. Bottom: differential Coulomb dissociation cross section with respect to excitation energy (E^*) of ^{17}C in coincidence with the 1.766 MeV γ transition ($^{16}C(2^+ \rightarrow 0^+)$). The smooth curves are the cross sections calculated on the basis of the direct-breakup model using plane-wave approximation for $l = 0$ and $l = 2$ neutrons (dotted curves) and their sum (solid curve). The dashed curve shows the result using the distorted-wave approximation.

and 0.03 for the last bound neutron if configurations of $^{16}C(0^+) \otimes \nu_{d_{5/2}}$ or $^{16}C(0^+) \otimes \nu_{d_{3/2}}$ are considered, respectively. The direct-breakup model yields a cross sections of 107 mb for a $^{16}C(0^+) \otimes \nu_d$ configuration with a spectroscopic factor of unity. Thus, our experimental result favors $I^\pi = 3/2^+$ as the ground-state spin of ^{17}C as its small ground-state spectroscopic factor results in a breakup cross section consistent with the experimental one. The same conclusion was drawn from the knockout reaction [26]. In Table 1, the experimental cross section for different core states and the cross sections predicted by the direct-breakup model are quoted. The spectroscopic factors for the neutron occupying different orbitals as predicted by the shell-model are also given. It should be noted, however, that the core excitation energies in the shell-model calculation are different from the experimentally known ones; for example, the first excited state appears at 2.369 MeV rather than at 1.766 MeV. Apart from the $I^\pi = 2^+$ state, the γ-ray spectrum in coincidence with the ^{16}C fragment exhibits a peak structure at sum-energy of around 3–4 MeV, see Fig. 2. The low counting statistics does not allow a quantitative analysis.

In conclusion, it has been shown that Coulomb dissociation is a tool well suited for exploring single-particle properties of exotic nuclei with loosely-bound valence nucleons. The electromagnetic interaction is especially sensitive to nuclei with valence neutrons occupying s orbitals. By means of a coincident observation of the core fragment, the released neutrons, and γ-rays emitted from the fragments, spectroscopic factors for ^{15,17}C ground-state configurations have been deduced. For ^{15}C, the main ground state configuration is found to be $^{14}C(0^+) \otimes \nu_s$. For ^{17}C, the dominant ground state configuration involves a mixture of s and d wave neutrons coupled to the first excited state of the ^{16}C core; a ground state spin $I^\pi = 1/2^+$ can be excluded. A comparison of the deduced spectroscopic factors with available data from other experimental methods proves that a quantitative assessment is feasible. The observed low-lying dipole strength in these neutron-rich carbon isotopes can be understood as a direct-breakup mechanism. It is found, however, that the description of the differential cross section within a distorted-wave approximation is not fully satisfactory. More systematical theoretical and experimental work is required in order to establish optical potentials appropriate to these neutron-rich nuclei.

Acknowledgements

The authors are thankful to Prof. A. Brown, NSCL, MSU for providing us with the results of his shell-model calculations.

This work was supported by the German Federal Minister for Education and Research (BMBF) under Contracts 06 OF 838 and 06 MZ 864, and by GSI via Hochschulzusammenarbeitsvereinbarungen under Contracts OFELZK, MZKRAK, and partly supported by the Polish Committee of Scientific Research under Contract No. 2PB03 144 18. Support

was received in part by DAAD/CAPES cooperative agreement No. 415-bra-probral/bu, CNPq and the MCT/FINEP/CNPq(Pronex) under contract No. 41.96. 0886.00 and FAPESP.

References

[1] P.G. Hansen, A.S. Jensen, B. Jonson, Annu. Rev. Nucl. Part. Sci. 45 (1995) 591.
[2] I. Tanihata, Nucl. Phys. A 654 (1999) 235c.
[3] T. Glasmacher, Annu. Rev. Nucl. Part. Sci. 48 (1998) 1.
[4] T. Aumann, et al., Phys. Rev. C 59 (1999) 1252.
[5] D. Sackett, et al., Phys. Rev. C 48 (1993) 118.
[6] F. Shimoura, et al., Phys. Lett. B 348 (1995) 29.
[7] M. Zinser, et al., Nucl. Phys. A 619 (1997) 151.
[8] T. Nakamura, et al., Phys. Lett. B 331 (1994) 296.
[9] T. Nakamura, et al., Phys. Rev. Lett. 83 (1999) 1112.
[10] A. Leistenschneider, et al., Phys. Rev. Lett. 86 (2001) 5542.
[11] Y. Suzuki, K. Ikeda, H. Salto, Prog. Theor. Phys. 83 (1990) 180.
[12] F. Catara, C.H. Dasso, A. Vitturi, Nucl. Phys. A 602 (1996) 181.
[13] T. Baumann, et al., Phys. Lett. B 439 (1998) 256.
[14] D. Bazin, et al., Phys. Rev. C 57 (1998) 2156.
[15] A. Navin, et al., Phys. Rev. Lett. 81 (1998) 5089.
[16] T. Aumann, et al., Phys. Rev. Lett. 84 (2000) 35.
[17] E. Sauvan, et al., Phys. Lett. B 491 (2000) 1.
[18] G. Murillo, S. Sen, S.E. Darden, Nucl. Phys. A 579 (1994) 125.
[19] J.D. Goss, et al., Phys. Rev. C 12 (1975) 1730.
[20] F.E. Cecil, et al., Nucl. Phys. A 255 (1975) 243.
[21] A. Ozawa, Nucl. Phys. A 691 (2001) 599.
[22] L. Chulkov, Nucl. Phys. A 674 (2000) 330.
[23] E.K. Warburton, D.J. Millener, Phys. Rev. C 39 (1992) 1120.
[24] M.S. Curtin, et al., Phys. Rev. Lett. 56 (1986) 34.
[25] D. Cortina-Gil, et al., Eur. Phys. J. A 10 (2001) 49.
[26] V. Maddalena, et al., Phys. Rev. C 63 (2001) 024613.
[27] D. Ridikas, et al., Nucl. Phys. A 628 (1998) 363.
[28] R. Chatterjee, et al., Nucl. Phys. A 675 (2000) 477.
[29] P. Descouvemont, et al., Nucl. Phys. A 675 (2000) 559.
[30] Yu.L. Parfenova, et al., Phys. Rev. C 62 (2000) 044602.
[31] H. Geissel, et al., Nucl. Instrum. Methods B 70 (1992) 286.
[32] J. Cub, et al., Nucl. Instrum. Methods A 402 (1998) 67.
[33] T. Blaich, et al., Nucl. Instrum. Methods A 314 (1992) 136.
[34] GEANT, Cern Library Long Writeup W5013, 1994.
[35] T. Aumann, et al., Nucl. Phys. A 649 (1999) 297c.
[36] A. Winther, K. Alder, Nucl. Phys. A 319 (1979) 518.
[37] C.A. Bertulani, G. Baur, Phys. Rep. 163 (1988) 299.
[38] D. Wilmore, P.E. Hodgson, Nucl. Phys. 55 (1964) 673.
[39] M.B. Chadwick, P.G. Young, Nucl. Sci. Engrg. 123 (1996) 17.
[40] B.A. Brown, private communication.
[41] F. Ajzenberg-Selove, Nucl. Phys. A 523 (1991) 1.
[42] D.R. Tilley, H.R. Weller, C.M. Cheves, Nucl. Phys. A 564 (1993) 1.